J Therm Anal Calorim (2009) 98:717–723
DOI 10.1007/s10973-009-0109-1

Rapid synthesis, kinetics and thermodynamics of binary $Mn_{0.5}Ca_{0.5}(H_2PO_4)_2 \cdot H_2O$

Banjong Boonchom · Chanaiporn Danvirutai

Received: 19 November 2008 / Accepted: 24 February 2009 / Published online: 28 July 2009

Abstract The binary manganese and calcium dihydrogen phosphate monohydrate $Mn_{0.5}Ca_{0.5}(H_2PO_4)_2 \cdot H_2O$ was synthesized by a rapid and simple co-precipitation method using phosphoric acid, manganese metal, and calcium carbonate at ambient temperature. Thermal transformation shows complex processes and the final decomposed product was the binary manganese calcium cyclotetraphosphate $MnCaP_4O_{12}$. The activation energies of some decomposed steps were calculated by Kissinger method. Activated complex theory has been applied to each step of the reactions and the thermodynamic functions are calculated. These values for transformation stages showed that they are non-spontaneous processes without the introduction of heat. The differences of physical and chemical properties of the synthesized compound and its decomposed product are compared with $M(H_2PO_4)_2 \cdot H_2O$ and $M_2P_4O_{12}$ (M = Mn and Ca), which indicate the effects of the presence of Ca ions in substitution of Mn ions and confirm the formation of solid solution.

B. Boonchom
King Mongkut's Institute of Technology Ladkrabang, Chumphon Campus, 17/1 M.6 Pha Thiew District, Chumphon 86160, Thailand

B. Boonchom (✉)
Department of Chemistry, Faculty of Science, King Mongkut's Institute of Technology Ladkrabang, Ladkrabang, Bangkok 10520, Thailand
e-mail: kbbanjon@kmitl.ac.th

C. Danvirutai
Department of Chemistry, Faculty of Science, Khon Kaen University, Khon Kaen 40002, Thailand

Keywords Kinetics · Thermodynamics · Manganese and calcium dihydrogen phosphate · A rapid co-precipitation

Introduction

Binary metal (II) dihydrogen phosphates have been continuously reported to be the important inorganic compounds because they have been widely applied as fertilizers, pigments for paint finishes for protection of metal, and fire retardants in paints or plastics [1–6]. Many binary metal (II) dihydrogen phosphates ($M_{1-x}A_x(H_2PO_4)_2 \cdot xH_2O$; where M and A = Ca, Mg, Mn, Fe, Co, Ni, Cu, or Zn) were reported on the thermal analysis (TA) under quasi-isothermal and quasi-isobaric conditions to follow the mechanism of dehydration [7–12]. They are transformed to binary metal (II) cyclo-tetraphosphates ($M_{1-x}A_xP_4O_{12}$ where $0 < x < 2$) by decomposition and dehydration reactions at high temperatures [6, 10–13]. All compounds are a good source for macro- (P) and micronutrients (Ca, Mg, Fe, Mn, Co, and Ni) fertilizers due to their solubility in soils. Additionally, $M_{1-x}A_xP_4O_{12}$ compounds have been widely applied as pigments, catalysts, and luminophore-supporting matrices [13–17]. Both $M_{1-x}A_x(H_2PO_4)_2 \cdot xH_2O$ and $M_{1-x}A_xP_4O_{12}$ compounds are isostructural with the singles of the corresponding metal dihydrogen phosphates and the corresponding metal (II) cyclo-tetraphosphates, respectively. Consequently, they have similar X-ray diffraction patterns and close unit cell parameters, which crystallize in monoclinic space group $P2_1/n$ ($Z = 2$) for the dihydrogen phosphate group and C2/c ($Z = 4$) for cyclo-tetraphosphate group [18].

So far, single or binary metal dihydrogen phosphates were synthesized from corresponding metal (II) carbonate

and phosphoric acid at low temperature (313–353 K) with long time periods (2 = 60 h) [6, 18]. Brandová et al. reported the thermal transformation of $Mn_{0.5}Ca_{0.5}(H_2PO_4)_2 \cdot xH_2O$ to $MnCaP_4O_{12}$ [9, 13] but the synthetic route was not reported. In this respect, the goal of this work was to synthesize $Mn_{0.5}Ca_{0.5}(H_2PO_4)_2 \cdot H_2O$ by a rapid co-precipitation method at ambient temperature, which is a simple and cost effective route. Thermal transformation of $Mn_{0.5}Ca_{0.5}(H_2PO_4)_2 \cdot H_2O$ relates to the role of the water of crystallization and influences the intermolecular interactions (affecting the internal energy and enthalpy) and the crystalline disorder (entropy) [19–22], which influences the free energy, thermodynamic activity, solubility, stability, electrochemical and catalytic activity. Therefore, kinetic (E, A) and thermodynamic (ΔH^*, ΔS^*, ΔG^*) parameters of thermal transformation steps of studied compound were calculated by isoconversional kinetics of Kissinger method and the activated complex theory, respectively. The physical meanings of kinetic and thermodynamic parameters were discussed for the first time.

Experimental

Synthesis and characterization

The binary manganese and calcium dihydrogen phosphate monohydrate $Mn_{0.5}Ca_{0.5}(H_2PO_4)_2 \cdot H_2O$ compound was prepared by solution co-precipitation method using the corresponding metal sources (Mn(c; complexometric), 99.99%, Merck and $CaCO_3$, 99.99%, Merck) and phosphoric acid (86.4 wt% H_3PO_4, Merck) as starting materials. Following the procedure, about 0.5494 of Mn(c) and 1.0080 g of $CaCO_3$ (a mole ratio corresponding to the nominal composition of Mn:Ca ratio of 1.0:1.0) were dissolved in 70% H_3PO_4 (86.4 wt% H_3PO_4 dissolved in DI water) with continuous mechanical stirring at ambient temperature. The resulting solution was stirred until CO_2(g) and H_2(g) were completely evolved (15–30 min) and the nearly dry precipitate was obtained. Then 10 mL of acetone was added to allow highly crystalline product to be developed. The pale gray solid of $Mn_{0.5}Ca_{0.5}(H_2PO_4)_2 \cdot H_2O$ product was filtered by suction pump, washed with acetone until free from phosphate ion and dried in air. Thermal analysis measurements (thermogravimetry, TG; differential thermogravimetry, DTG; and differential thermal analysis, DTA) were carried out by a Pyris Diamond Perkin-Elmer apparatus by increasing the temperature from 303 to 773 K with calcined α-Al_2O_3 powder as the standard reference. The retained mass found to be occurred at temperatures above 673 K, so the prepared solid was consequently calcined in a box-furnace at 773 K for 2 h in air. The final product was obtained as white pink solid of $MnCaP_4O_{12}$. The manganese and calcium contents of the synthesized $Mn_{0.5}Ca_{0.5}(H_2PO_4)_2 \cdot H_2O$ and the decomposed product $MnCaP_4O_{12}$ were determined by atomic absorption spectrophotometer (AAS, Perkin-Elmer, Analyst100). The phosphorus content was determined by colorimetric analysis of the molybdophosphate complex. The structure of the prepared product and the calcined sample were studied by X-ray powder diffraction using a D8 Advanced powder diffractometer (Bruker AXS, Karlsruhe, Germany) with Cu $K\alpha$ radiation ($\lambda = 0.15406$ Å). The room temperature FTIR spectra were recorded in the range of 4000–370 cm^{-1} with eight scans on a Perkin-Elmer Spectrum GX FTIR/FT-Raman spectrometer with a resolution of 4 cm^{-1} using KBr pellets (spectroscopy grade, Merck). The particle sizes and external morphologies of the prepared sample and its decomposed powders were characterized by scanning electron microscope (SEM) using LEO SEM VP1450 after gold coating.

Kinetic and thermodynamic functions

To evaluate the activation energies for the thermal decomposition of $Mn_{0.5}Ca_{0.5}(H_2PO_4)_2 \cdot H_2O$, a TG–DTG–DTA Pyris Diamond Perkin-Elmer Instrument was used. The experiments were performed in air atmosphere at heating rates of 5, 10, 15, and 20 K min^{-1} over the temperature range from 303 to 873 K and the O_2 flow rate of 100 mL min^{-1}. The activation energies for the thermal transformation steps of $Mn_{0.5}Ca_{0.5}(H_2PO_4)_2 \cdot H_2O$ were calculated from peaks on the DTA curves using the Kissinger equation [23]:

$$\ln\left(\frac{\beta}{T_p^2}\right) = -\frac{E_a}{RT_p} + \ln\left(\frac{AR}{E_a}\right). \quad (1)$$

Here, β is the DTA scan rate (K min^{-1}), E_a is the activation energy for the phase transformation (kJmol^{-1}), R is the gas constant (8.314 Jmol^{-1} K^{-1}) and T_p is the phase transformation temperature peak in the DTA curve (K). The fact that the T_p values for various heating rates can be precisely evaluated from non-isothermal data (DTA, DTG or DSC curves) conferred to the Kissinger method to evaluate the kinetic parameters a high popularity. The plots of ln (β/T^2) versus $1/T_p$ should give the straight lines with the best correlation coefficients of the linear regression (R^2), which have been proved to give the values of activation energy and pre-exponential factor by the slope and the intercept for the different thermal transformation stages of $Mn_{0.5}Ca_{0.5}(H_2PO_4)_2 \cdot H_2O$. The advantage of Kissinger equation is that the values of E and A can be calculated on the basis of multiple thermogravimetric curves, which does not require selection of particular kinetic model (type of $g(\alpha)$ or $f(\alpha)$ functions) [24–27]. In addition, the E and A

values obtained by this method are usually regarded as more reliable than those obtained by a single thermogravimetric curve.

From the activated complex theory (transition state) of Eyring [11, 12, 19–21, 26, 27], the following general equation may be written:

$$A = \left(\frac{e\chi k_B T_{Ap}}{h}\right) \exp\left(\frac{\Delta S^*}{R}\right) \quad (2)$$

where A is the pre-exponential factor A obtained from the Kissinger method; e = 2.7183 is the Neper number; χ: transition factor, which is unity for monomolecular reactions; k_B: Boltzmann constant; h: Plank constant, and T_{Ap} is the average phase transformation temperature peak in four DTA curves (K). The change of the entropy may be calculated according to the formula:

$$\Delta S^* = R \ln\left(\frac{Ah}{e\chi k_B T_{Ap}}\right) \quad (3)$$

Since

$$\Delta H^* = E^* - RT_{Ap}, \quad (4)$$

$$\Delta G^* = \Delta H^* - T_{Ap}\Delta S^* \quad (5)$$

when E*is the activation energy E_a obtained from the Kissinger method. The changes of the enthalpy ΔH* and Gibbs free energy ΔG* for the activated complex formation from the reagent can be calculated using the well-known thermodynamic equation. In this article we suggested the relation between kinetic (E and A) and thermodynamic (ΔH*, ΔS*, and ΔG*) parameters of the thermal transformation of $Mn_{0.5}Ca_{0.5}(H_2PO_4)_2 \cdot H_2O$ based on Kissinger method, which was attracted the interesting of thermodynamic and kinetic scientists.

Results and discussion

Characterization results

The chemical analysis results of the synthesized sample and its decomposed product found to be wt% of Mn_{total}: Ca_{total}:P_{total}; 9.58:7.13:21.87 and 12.33:9.68:27.98, respectively. These results give rise the mole ratio of Mn_{total}: Ca_{total}:P_{total} = 1.00:1.02:4.05 for the synthesized sample and 1.00:1.08:4.02 for its decomposition product. The water content of the synthesized sample was analyzed by TG data and was about of 20.02 wt% (3.08 mol) H_2O. These results indicate that the general formula of the synthesized sample and its decomposition product would be $Mn_{0.5}Ca_{0.5}(H_2PO_4)_2 \cdot H_2O$ and $MnCaP_4O_{12}$.

The results of simultaneous TG–DTG–DTA analyses of the prepared $Mn_{0.5}Ca_{0.5}(H_2PO_4)_2 \cdot H_2O$ are shown in

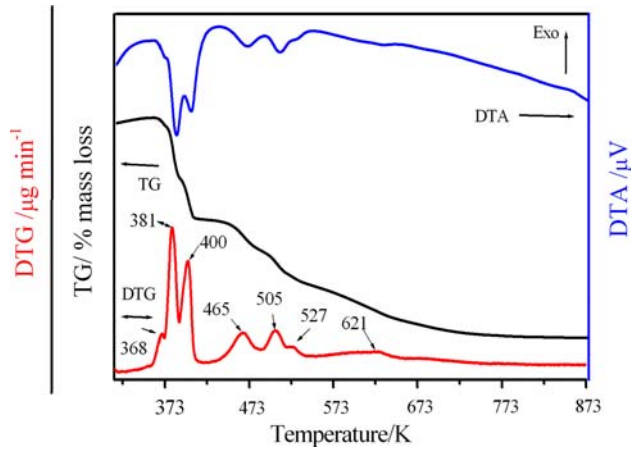

Fig. 1 TG–DTA–DTG curves of $Mn_{0.5}Ca_{0.5}H_2PO_4)_2 \cdot H_2O$ in the heating rate of 10 K min^{-1}

Fig. 1. The TG curve of $Mn_{0.5}Ca_{0.5}(H_2PO_4)_2 \cdot H_2O$ shows seven stages of the mass loss in the range of 323–873 K, which appear in the respective DTG and DTA as: 368, 381, 400, 465, 505, 527, and 621 K. A shoulder peak at 368 K on DTG and DTA curves (first step) corresponds to a minor mass loss in TG trace, which related to the loss of moisture for $Mn_{0.5}Ca_{0.5}(H_2PO_4)_2 \cdot H_2O$. The total mass loss is 20.02% (3.08 mol H_2O), which is close to the theoretical values (21.42% (3.00 mol H_2O) for $Ca(H_2PO_4)_2 \cdot H_2O$, 25.27% (4.00 mol H_2O) for $Mn(H_2PO_4)_2 \cdot 2H_2O$ and 20.81% (3.00 mol H_2O) for $Mn_{0.5}Ca_{0.5}(H_2PO_4)_2 \cdot H_2O$). This result is in agreement with other binary metal dihydrogen phosphate hydrates (isostructural compounds) in literatures, which reported the mole of water in the range of 1–4 [6–10]. The thermal decomposition of $Mn_{0.5}Ca_{0.5}(H_2PO_4)_2 \cdot H_2O$ is a complex process, which involves the dehydration of the coordinated water molecules (1 mol H_2O) and an intramolecular dehydration of the protonated phosphate groups (2 mol H_2O), these processes could formally be presented as:

$$Mn_{0.5}Ca_{0.5}(H_2PO_4)_2 \cdot H_2O \rightarrow Mn_{0.5}Ca_{0.5}(H_2PO_4)_2 \cdot 0.50H_2O + \sim 0.50H_2O \quad (6)$$

$$Mn_{0.5}Ca_{0.5}(H_2PO_4)_2 \cdot 0.50H_2O \rightarrow Mn_{0.5}Ca_{0.5}(H_2PO_4)_2 + \sim 0.50H_2O \quad (7)$$

$$Mn_{0.5}Ca_{0.5}(H_2PO_4)_2 \rightarrow 1/2(MnH_2P_2O_7 \cdot CaH_2P_2O_7) + \sim H_2O \quad (8)$$

$$(MnH_2P_2O_7 \cdot CaH_2P_2O_7) \rightarrow (1/2Mn_2P_4O_{12}) \cdot CaH_2P_2O_7 + 0.50H_2O \quad (9)$$

$$(1/2Mn_2P_4O_{12}) \cdot CaH_2P_2O_7 \rightarrow (1/2Mn_2P_4O_{12}) \cdot Ca(PO_3)_{2*} + 0.50H_2O \quad (10)$$

$$(1/2Mn_2P_4O_{12}) \cdot Ca(PO_3)_2 \rightarrow 1/2MnCaP_4O_{12} \quad (11)$$

The intermediate compounds; $Mn_{0.5}Ca_{0.5}(H_2PO_4)_2 \cdot 0.50\ H_2O$, $Mn_{0.5}Ca_{0.5}(H_2PO_4)_2$, $MnH_2P_2O_7 \cdot CaH_2P_2O_7$ ($Mn_{0.5}Ca_{0.5}H_2P_2O_7$), $(Mn_2P_4O_{12}) \cdot CaH_2P_2O_7$, $(Mn_2P_4O_{12}) \cdot Ca(PO_3)_2$ and mixing intermediates of all have been registered. The decomposed processes and the presented intermediates were similarly observed with other binary dihydrogen phosphates [8–12]. The binary manganese calcium cyclotetraphosphate, $MnCaP_4O_{12}$ is found to be the final product of the thermal decomposition at $T > 673$ K. The different thermal behavior between the synthesized $Mn_{0.5}Ca_{0.5}(H_2PO_4)_2 \cdot H_2O$ and the individual $Mn(H_2PO_4)_2 \cdot 2H_2O$ [6, 9, 19] or $Ca(H_2PO_4)_2 \cdot H_2O$ [9] confirms the formation of a binary $Mn_{0.5}Ca_{0.5}(H_2PO_4)_2 \cdot H_2O$. Additionally, this synthesized compound shows different thermal behavior from that of the Brandová research [9], which this may be the differences of water content and preparation methods. Based on these results, we can conclude that the different thermal behavior is affected by the incorporation of Mn and Ca metals in the skeleton, which the conclusion was confirmed by XRD and FTIR data (Figs. 2, 3).

The XRD patterns of $Mn_{0.5}Ca_{0.5}(H_2PO_4)_2 \cdot H_2O$ and $MnCaP_4O_{12}$ are similar to those of $Mn(H_2PO_4)_2 \cdot 2H_2O$ and $Mn_2P_4O_{12}$, respectively (Fig. 2) [6, 19]. In the systems of binary manganese calcium solid solutions and individual metal dihydrogen phosphate (or metal cyclotetraphosphate), the electric charges of cations are equivalent, and the radii of cations are close to each other, so the spectrum peaks are quite similar [6, 18, 19]. However, the XRD peaks of $Mn_{0.5}Ca_{0.5}(H_2PO_4)_2 \cdot H_2O$ and $MnCaP_4O_{12}$ exhibit lower intensity and broader peaks than those of $Mn(H_2PO_4)_2 \cdot 2H_2O$ and $Mn_2P_4O_{12}$, which indicate poor crystallinity after

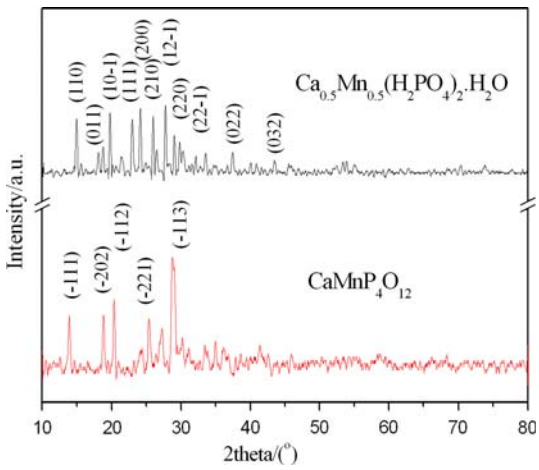

Fig. 2 XRD patterns of $Mn_{0.5}Ca_{0.5}H_2PO_4)_2 \cdot H_2O$ and $MnCaP_4O_{12}$

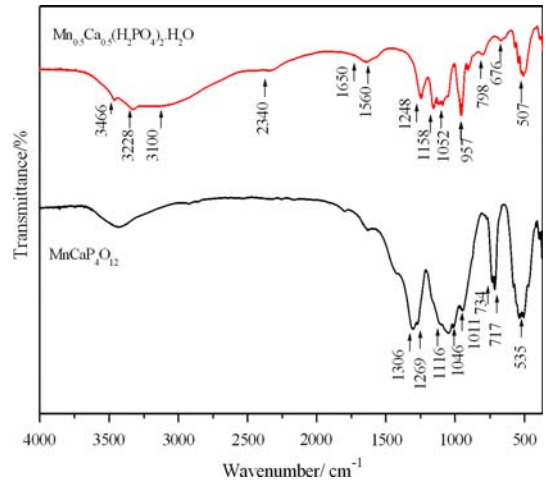

Fig. 3 FTIR spectra of $Mn_{0.5}Ca_{0.5}H_2PO_4)_2 \cdot H_2O$ and $MnCaP_4O_{12}$

obtaining the mixed binary products. Based on the above analysis, we can draw a conclusion that the synthesized $Mn_{0.5}Ca_{0.5}(H_2PO_4)_2 \cdot H_2O$ and its decomposed product $MnCaP_4O_{12}$ are solid solutions that are not a mixture of single phase of Mn and Ca. XRD results confirm that a binary $Mn_{0.5}Ca_{0.5}(H_2PO_4)_2 \cdot H_2O$ and $MnCaP_4O_{12}$ are isostructural with the type series of $M(H_2PO_4)_2 \cdot 2H_2O$ and $M_2P_4O_{12}$ (M = Mg, Mn, Co, Ni, Fe, and Zn), respectively. Consequently, all reflections can be distinctly indexed based on a pure monoclinic of single phase with space group $P2_1/n$ ($Z = 2$) for $Mn_{0.5}Ca_{0.5}(H_2PO_4)_2 \cdot H_2O$ and C2/c ($Z = 4$) for $MnCaP_4O_{12}$, which note to be similar to those of the standard XRD patterns of $Mn(H_2PO_4)_2 \cdot 2H_2O$ (PDF#350010) and $Mn_2P_4O_{12}$ (PDF#380314), respectively. The average crystallite sizes and lattice parameters of $Mn_{0.5}Ca_{0.5}(H_2PO_4)_2 \cdot H_2O$ and $MnCaP_4O_{12}$ samples were calculated from XRD line broadening and tabulated in Table 1. Their lattice parameters are comparable to those of the standard data as $M(H_2PO_4)_2 \cdot nH_2O$, (PDF#350010 for Mn and PDF#0903047 for Ca), $Mn_2P_4O_{12}$ (PDF#380314) and $Ca(PO_3)_2$ (PDF#500584), respectively.

The FTIR spectra of $Mn_{0.5}Ca_{0.5}(H_2PO_4)_2 \cdot H_2O$ and $MnCaP_4O_{12}$ are shown in Fig. 3, which are very similar to those of $Mn(H_2PO_4)_2 \cdot 2H_2O$ and $Mn_2P_4O_{12}$ [19, 28]. Vibrational bands are identified in relation to the crystal structure in terms of the fundamental vibrating units namely $H_2PO_4^-$ and H_2O for $Mn_{0.5}Ca_{0.5}(H_2PO_4)_2 \cdot H_2O$ and $[P_4O_{12}]^{4-}$ ion for $MnCaP_4O_{12}$, which are assigned according to the literatures [19, 24, 25, 28, 29]. Vibrational bands of $H_2PO_4^{-2}$ ion are observed in the regions of 300–500, 700–900, 1160–900, 840–930, 1000–1200, 2300–2400, 2800–3120, and 3200–3500 cm^{-1}. These bands are assigned to the $\delta(PO_3)$, $\gamma(POH)$, $\delta(POH)$, $\nu(PO_2(OH))$, $\nu(PO_3)$, B band (ν_{OH} HPO_4^{-2}), A band (ν_{OH} HPO_4^{-2}) and ν_{OH} (ν_1 and ν_3 H_2O), respectively. The observed bands in 1600–1700 cm^{-1}

Table 1 Average crystallite sizes and lattice parameters of $Mn_{0.5}Ca_{0.5}H_2PO_4)_2 \cdot H_2O$ and $MnCaP_4O_{12}$ calculated from XRD data

Compound	Method	*a* (Å)	*b* (Å)	*c* (Å)	*β* (°)	Average crystallite sizes (nm)
$Mn(H_2PO_4)_2 \cdot 2H_2O$	PDF#350010	7.31	10.08	5.37	94.75	–
$MnCa(H_2PO_4)_2 \cdot H_2O$	This work	7.92 (0)	10.62 (4)	5.79 (4)	94.68 (6)	27 ± 8
$Ca(H_2PO_4)_2 \cdot H_2O$	PDF#0903047	6.25	11.89	5.63	114.20	
$Mn_2P_4O_{12}$	PDF#380314	11.88	8.59	10.14	119.21	–
$MnCaP_4O_{12}$	This work	12.27 (9)	8.87 (2)	10.49 (8)	120.00 (2)	30 ± 9
$Ca(PO_3)_2$	PDF#500584	9.56	9.50	10.37	93.47	

region are attributed to the water bending/C band. The P–O stretching modes of the $[P_4O_{12}]^{4-}$ anion are known to appear in the 1150–960 cm^{-1} region [19, 28]. The one of the most noteworthy features of the spectra is the presence of strong bands in the ranges of 1350–1220, 1150–1100, 1080–950, and 780–400 cm^{-1}. These bands can be assigned to $\nu_{as}OPO^-$, ν_sOPO^-, $\nu_{as}POP$, and ν_sPOP vibrations, respectively [19, 28]. The two doublet bands around 720 (ca. 734 and 717 cm^{-1}) and 1280 (ca. 1306 and 1269 cm^{-1}) cm^{-1} are observed in the FTIR spectra of $Mn_2P_4O_{12}$ and $MnCaP_4O_{12}$ and assigned to ν_sPOP vibrations. The observation of a strong ν_sPOP band is known to be the most striking feature of cyclotetraphosphate spectra, along with the presence of the $\nu_{as}OPO^-$ band, which is different from that of polyphosphate. From X-ray diffraction data [30], it was shown that the crystal structure is monoclinic (space group C2/c) with a cyclic structure of the $[P_4O_{12}]^{4-}$ anion, which was confirmed by the FTIR measurements.

The scanning electron micrographs of $Mn_{0.5}Ca_{0.5}(H_2PO_4)_2 \cdot H_2O$ and their final decomposition product $MnCa\ P_4O_{12}$ show different morphological features and high aggregates (Fig. 4). The SEM micrograph of $Mn_{0.5}Ca_{0.5}(H_2PO_4)_2 \cdot H_2O$ shows roughness of many small and some large boundary surfaces, which indicate amorphous morphology by inferring from XRD evidence to be poorly-crystalline $Mn_{0.5}Ca_{0.5}(H_2PO_4)_2 \cdot H_2O$. In addition, $MnCaP_4O_{12}$ shows similarly morphological feature to that of $Ca(PO_3)_2$, which illustrates more aggregate of small particles and large spherical particles. Based on the SEM results, the SEM micrographs of $Mn_{0.5}Ca_{0.5}(H_2PO_4)_2 \cdot H_2O$ and $MnCaP_4O_{12}$ powders appear to be highly agglomerated

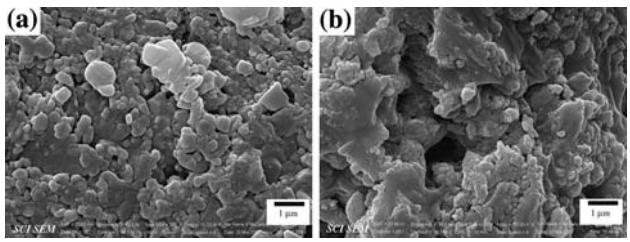

Fig. 4 SEM micrographs of $Mn_{0.5}Ca_{0.5}H_2PO_4)_2 \cdot H_2O$ (**a**) and $MnCaP_4O_{12}$ (**b**)

caused primarily by the process of dissolution, a rapid precipitation and decomposition process, respectively. The particles sizes of $Mn_{0.5}Ca_{0.5}(H_2PO_4)_2 \cdot H_2O$ and $MnCa\ P_4O_{12}$ appear smaller than those of the individual $M(H_2PO_4)_2 \cdot 2H_2O$ and $M_2P_4O_{12}$, which are well consistent with the results of XRD [19, 28].

Kinetic and thermodynamic results

According to Kissinger method, the basic data of *T* collected from the DTA curves of the decomposition of $Mn_{0.5}Ca_{0.5}(H_2PO_4)_2 \cdot H_2O$ at various heating rates of 5, 10, 15, and 20 K min^{-1}. Kinetics studies of $Mn_{0.5}Ca_{0.5}(H_2PO_4)_2 \cdot H_2O$ were only analyzed five steps (1st, 2nd, 3rd, 4th, and 6th) because the 5th step were not observed in the heating rates of 15 and 20 K min^{-1}. According to the Kissinger Eq. 1, the plots of ln β/T^2 versus $1000/T$ can be obtained by a linear regression of least-square method. Non-isothermal DTA method is desirable to analyze the reaction mechanism and calculates the activation energy of the solid state transformations [23, 31–33]. Several non-isothermal techniques have been proposed which are quicker and less sensitive to previous and next transformations. In addition, they can provide the more accurate activation energy and crystal growth mode. From the slopes of the Kissinger plots, the activation energy values in five decomposed steps of the prepared $Mn_{0.5}Ca_{0.5}(H_2PO_4)_2 \cdot H_2O$ were determined as shown in Table 2. These activation energies are consistent with the former hypothesis that the intermediate nucleate and crystallize as metastable phase with adequate growth kinetics before the stable phase $MnCaP_4O_{12}$. The last and third steps exhibit higher and lower activation energies in comparison with the other ones, respectively. The reason may be relevant to the strengths of binding of water molecules in the crystal lattice. Hence, different dehydration temperatures and kinetic parameters are expected. The activation energy for the release of crystal water lie in the range of 50–130 kJ mol^{-1}, while the value for coordinately bounded one are higher than this range [20–22]. The energy of activation found in the range of 89–236 kJ mol^{-1} for the five decomposition reactions

Table 2 Values of ΔS^*, ΔH^* and ΔG^* for five decomposition steps of $Mn_{0.5}Ca_{0.5}(H_2PO_2)_4 \cdot H_2O$

Parameter	1st step	2nd step	3rd step	4th step	6th step
R^2	0.9929	0.9942	0.9996	0.9995	0.9567
E_a (kJmol^{-1})	147.85 ± 13	129.70 ± 10	89.41 ± 2	152.94 ± 4	236.97 ± 51
A (s^{-1})	1.41×10^{20}	6.55×10^{16}	4.48×10^{9}	4.04×10^{15}	1.01×10^{20}
ΔS^* (J mol^{-1} K^{-1})	130.34	66.18	−72.26	41.10	123.73
ΔH^* (kJmol^{-1})	144.65	126.35	85.50	148.71	231.85
ΔG^* (kJmol^{-1})	94.38	99.64	119.53	127.80	155.59

Fifth step was not observed in the heating rates of 15 and 20 K min^{-1}

suggest that the water molecules are coordinately linked water as well as crystal one. The five mass loss steps correspond to the loss of water of coordinated-water in the first two steps, subsequently to a continuous intermolecular polycondensation and the elimination of water of constituent in anion in the last three steps [19, 22].

The pre-exponential factor (A) can be estimated from the intercept of the plots of Eq. 1 (Table 2). All calculations were performed using a programs complied by ourselves. The pre-exponential factor (A) values in Arrhenius equation for solid phase reactions are expected to be in a wide range (six or seven orders of magnitude), even after the effect of surface area is taken into account [24, 25]. The low factors will often indicate a surface reaction, but if the reactions are not dependent on surface area, the low factor may indicate a "tight" complex. The high factors will usually indicate a "loose" complex. Even higher factors (after correction for surface area) can be obtained for complexes having free translation on the surface. Since in many cases the concentrations in solids are not controllable, it would have been convenient if the magnitude of the pre-exponential factor can provide the information for the reaction molecularity. Such a bulk decomposition, any molecule is as likely as to react with any others; and no preference is shown toward corners, edges, surface, defects or sites of previous decomposition. On the basis of these reasons, the thermal decomposition reaction of $Mn_{0.5}Ca_{0.5}(H_2PO_4)_2 \cdot H_2O$ may be interpreted as "loose complexes" for 1st, 2nd, 4th and 6th step and "tight complexes" for 3rd step, which correspond to the proposed reaction in (Eqs. 1–4 and 6).

As can be seen from Table 2, the entropy of activation (ΔS^*) values for all steps are positive values. It means that the corresponding activated complexes had lower degrees of arrangement than the initial state. Since the decomposition of $Mn_{0.5}Ca_{0.5}(H_2PO_4)_2 \cdot H_2O$ proceeds as five consecutive reactions, the formation of the 2nd, 3rd, 4th, and 6th activated complex passed in situ. In the terms of the activated complex theory (transition theory), [11, 12, 19–21, 26, 27, 29] a positive value of ΔS^* indicates a malleable activated complex that leads to a large number of degrees of freedom of rotation and vibration. A result may be interpreted as a ''fast'' stage. On the other hand, a negative value of ΔS^* indicates a highly ordered activated complex and the degrees of freedom of rotation as well as of vibration are less than they are in the non activated complex. These results may indicate a ''slow'' stage [19–21]. In respect of these results, 1st, 2nd, 4th and 6th decomposed steps of $Mn_{0.5}Ca_{0.5}(H_2PO_4)_2 \cdot H_2O$ may be interpreted as ''fast'' stages whereas 3rd decomposed step may be interpreted as "slow" stage. The positive values of the enthalpy ΔH^* are in good agreement with five endothermic effects in DTA data. The positive values of ΔH^* and ΔG^* for all stages show that they are connected with the introduction of heat and are non-spontaneous processes.

Conclusions

$Mn_{0.5}Ca_{0.5}(H_2PO_4)_2 \cdot H_2O$ was successfully synthesized by a rapid and simple precipitation using phosphoric acid, manganese metal, and calcium carbonate at ambient temperature. The different chemical and physical properties of binary compounds ($Mn_{0.5}Ca_{0.5}(H_2PO_4)_2 \cdot H_2O$ and MnCa P_4O_{12}) and the individual ones ($M(H_2PO_4)_2 \cdot nH_2O$ (M = Mn and Ca) and $Mn_2P_4O_{12}$ or $Ca(PO_3)_2$) were revealed by FTIR, XRD, and SEM techniques. Kinetic analysis from non-isothermal DTA applying KAS method results exhibits the activation energies (E) in five decomposition steps, which correspond to the loss of water of crystallization (the first two steps), subsequently to a continuous intermolecular polycondensation and elimination of water of constituent in anion (the last three steps). On the basis of correctly established values of the apparent activation energy, pre-exponential factor and the changes of entropy, enthalpy and Gibbs free energy, certain conclusions can be made concerning the mechanisms and characteristics of the processes. Thus, various scientific and practical problems involving the participation of solid phases can be solved.

Acknowledgements The authors would like to thank the Chemistry Department, Khon Kaen University for facilities. This work is financially supported by the Thailand Research Fund (TRF) and the Commission on Higher Education (CHE): Research Grant for New Scholar (MRG52_Banjong Boonchom) and King Mongkut's Institute of Technology Ladkrabang Research (KMITL Research), Ministry of Science and Technology, Thailand.

References

1. Jouini A, Gâcon JC, Ferid M, Trabelsi-Ayadi ML. Luminescence and scintillation properties of praseodymium poly and diphosphates. Opt Mater. 2003;24:175–80.
2. Kitsugi T, Yamamuro T, Nakamura T, Oka M. Transmission electron microscopy observations at the interface of bone and four types of calcium phosphate ceramics with different calcium/phosphorus molar ratios. Biomaterials. 1995;16:1101–7.
3. Jian-Jiang B, Dong-Wan K, Kug Sun H. Microwave dielectric properties of $Ca_2P_2O_7$. J Eur Ceram Soc. 2003;23:2589–92.
4. Kaplanová M, Trojan M, Brandová D, Navrátil J. On the luminescence on manganese(II) phosphates. J Lumin. 1984;29:199–204.
5. Wang C-M, Liau H-C, Tsai W-T. Effect of heat treatment on the microstructure and electrochemical behavior of manganese phosphate coating. Mater Chem Phys. 2007;102:207–13.
6. Antraptseva NM, Shchegrov LN, Ponomareva IG. Thermolysis features of manganese(II) and zinc dihydrogenphosphate solid solution. Russ J Inorg Chem. 2006;51:1493–7.
7. Trojan M, Brandová D, Paulik F, Arnold M. Mechanism of the thermal dehydration of $Co_{1/2}Ca_{1/2}(H_2PO_4)_2{\cdot}2H_2O$. J Therm Anal Calorim. 1990;36:929–38.
8. Trojan M, Brandová D. Mechanism of dehydration of $Zn_{0.5}Mg_{0.5}(H_2PO_4)_2{\cdot}2H_2O$. Thermochim Acta. 1990;159:1–12.
9. Brandová D, Trojan M, Paulik F, Paulik J, Arnold M. Study of the thermal dehydration of $Mn_{1/2}Ca_{1/2}(H_2PO_4)_2{\cdot}2H_2O$. J Therm Anal Calorim. 1990;36:881–9.
10. Trojan M, Brandová D. Study of thermal dehydration of $Mn_{0.5}Mg_{0.5}(H_2PO_4)_2{\cdot}4H_2O$. Thermochim Acta. 1990;161:11–21.
11. Brandová D, Trojan M. Mechanism of dehydration of $Zn_{0.5}Mg_{0.5}(H_2PO_4)_2{\cdot}2H_2O$. Thermochim Acta. 1990;157:1–9.
12. Trojan M, Brandová D, Šolc Z. Study of the thermal preparation and stability of tetrametaphosphates of bivalent metals. Thermochim Acta. 1987;110:343–8.
13. Trojan M. Double tetrametaphosphates $Mn_{2-x}Ca_xP_4O_{12}$ as special pigments. Dye Pigment. 1990;12:35–47.
14. Trojan M. Binary cyclotetraphosphates $Zn_{2-x}Ca_xP_4O_{12}$ as new special pigments. Dye Pigment. 1990;13:1–10.
15. Trojan M, Šulcová P, MoŠner P. The synthesis of binary zinc(II)−nickel(II)cyclo-tetraphosphates as new special pigments. Dye Pigment. 2000;44:161–4.
16. Trojan M, Brandová D. A study of the thermal preparation of c-$Cd_{4/3}Ca_{2/3}P_4O_{12}$. Thermochim Acta. 1990;160:349–59.
17. Trojan M, Šulcová P. Binary Cu(II)−Mn(II) cyclo-tetraphosphates. Dye Pigment. 2000;47:291–4.
18. Viter VN, Nagornyi PG. Synthesis of continuous substitutional solid solutions $M_{1-x}Ni_x(H_2PO_4)_2{\cdot}2H_2O$ with M = Mg, Mn, Co, or Zn. Russ J Inorg Chem. 2007;52:14–20.
19. Boonchom B, Maensiri S, Danvirutai C. Soft solution synthesis, non-isothermal decomposition kinetics and characterization of manganese dihydrogen phosphate dihydrate $(H_2PO_4)_2{\cdot}2H_2O$ and its thermal transformation products. Mater Chem Phys. 2008;109: 404–10.
20. Boonchom B, Youngme S, Danvirutai C. A rapid co-precipitation and non-isothermal decomposition kinetics of new binary $Mn_{0.5}Co_{0.5}(H_2PO_4)_2{\cdot}2H_2O$. Solid State Sci. 2008;10:129–36.
21. Gabal MA. Kinetics of the thermal decomposition of CuC_2O_4−ZnC_2O_4 mixture in air. Thermochim Acta. 2003;402:199–208.
22. Gao X, Dollimore D. The thermal decomposition of oxalates. Part 26: a kinetic study of the thermal decomposition of manganese (II) oxalate dihydrate. Thermochim Acta. 1993;215:47–63.
23. Kissinger HE. Reaction kinetics in differential thermal analysis. Anal Chem. 1957;29:1702–6.
24. Singh BK, Sharma RK, Garg BS. Kinetics and molecular modeling of biologically active glutathione complexes with lead(II) ions. J Therm Anal Calorim. 2006;84:593–600.
25. Vlaev L, Nedelchev N, Gyurova K, Zagorcheva M. A comparative study of non-isothermal kinetics of decomposition of calcium oxalate monohydrate. J Anal Appl Pyrolysis. 2008;81:253–62.
26. Vlase T, Jurca G, Doca N. Non-isothermal kinetics by decomposition of some catalyst precursors. Thermochim Acta. 2001; 379:65–9.
27. Vlase T, Vlase G, Doca M, Doca N. Specificity of decomposition of solids in non-isothermal conditions. J Therm Anal Calorim. 2003;72:597–604.
28. Soumhi EH, Saadoune I, Driss A. A new organic-cation cyclotetraphosphate $C_{10}H_{28}N_4P_4O_{12}{\cdot}4H_2O$: crystal structure, thermal analysis, and vibrational spectra. J Solid State Chem. 2001;156: 364–9.
29. Koleva V, Effenberger H. Crystal chemistry of $M[PO_2(OH)_2]_2{\cdot}2H_2O$ compounds (M = Mg, Mn, Fe, Co, Ni, Zn, Cd): structural investigation of the Ni, Zn and Cd salts. J Solid Sate Chem. 2007;180:956–67.
30. Bagieu-Beucher M, Gondrand M, Perroux M. Etude à haute pression des tétramétaphosphates du type $M_2P_4O_{12}$ (M = Ni, Mg, Cu, Co, Fe, Mn, Cd). Données cristallographiques sur tous les composés $M_2P_4O_{12}$. J Solid State Chem. 1967;19:353–7.
31. Hong J, Guo G, Zhang Z. Kinetics and mechanism of non-isothermal dehydration of nickel acetate tetrahydrate in air. J Anal Appl Pyrolysis. 2006;77:111–5.
32. Ioiţescu A, Vlase G, Vlase T, Doca N. Thermal behaviour of some industrial and food dyes. J Therm Anal Calorim. 2007;88: 121–5.
33. Gabal MA, El-Bellihi AA, Ata-Allah SS. Effect of calcination temperature on Co(II) oxalate dihydrate−iron(II) oxalate dihydrate mixture DTA− TG, XRD, Mössbauer, FT-IR and SEM studies (Part II). Mater Chem Phys. 2003;81:84–92.